Carbohydrate Polymers 101 (2014) 1074–1080

Contents lists available at ScienceDirect

Carbohydrate Polymers

journal homepage: www.elsevier.com/locate/carbpol

Composition and physicochemical properties of Zedo gum exudates from *Amygdalus scoparia*

Ghasem Fadavi, Mohammad Amin Mohammadifar*, Azizollaah Zargarran, Amir Mohammad Mortazavian, Rozita Komeili

Department of Food Science and Technology, National Nutrition and Food Technology Research Institute, Faculty of Nutrition Sciences and Food Technology, Shahid Beheshti University of Medical Sciences, P.O. Box 19395-4741, Tehran, Iran

ARTICLE INFO

Article history:
Received 8 August 2013
Received in revised form
27 September 2013
Accepted 29 September 2013
Available online 6 October 2013

Keywords:
Amygdalus scoparia
Arabinogalactan
Rheology
Thermal analysis
Sugar composition
GPC–MALLS

ABSTRACT

Composition and physicochemical properties of three types of Zedo gum exudates from *Amygdalus scoparia* were investigated. Monosaccharide analysis by GC–MS indicated the occurrence of arabinose and galactose as the main sugars. FTIR spectra showed no differences in functional groups among the samples. Steady shear rheological data and power law parameters revealed that the white gum (W) was the most shear sensitive type and had the highest value of consistency coefficient. The mechanical spectra derived from the strain and frequency sweep measurements indicated a liquid viscoelastic behavior for Zedo gum dispersions. GPC–MALLS revealed that the white sample had the highest apparent average molecular weight (4.74×10^6 Da) and the lowest dispersity (1.045). TG–DTA analysis showed that the character of gum decomposition significantly depended on the gum type and the white sample had the highest thermal stability.

1. Introduction

Over the past few years, food industries have been evolved in terms of technologies in order to respond to new consumer trends (e.g., fast foods, health and diversity) and their products have become increasingly sophisticated. Polysaccharides can provide a unique opportunity for new food formulations and play a key role in food products as thickeners, gelling agents, emulsifiers and stabilizers (Persin et al., 2011).

The great diversity in the structural features of polysaccharides, originated from differences in monosaccharide composition, polymerization degree, linkage types, and functional groups dictates their physical properties, including solubility, flow behavior and surface and interfacial properties. This diversity also leads to unique functional roles exhibited by each polysaccharide. Thus, any advances in the use of polysaccharides are closely linked to knowledge of the structure–function relationships (Cui, 2005). In recent decades, many researchers have paid attention to studying new polysaccharides, due to the possibility of their application in a wide range of fields, especially food industries (Fan et al., 2012; Luo, Sun, Wu, & Yang, 2012).

Zedo gum (also called Farsi gum) exudes in three colors (white, yellow and red) from the trunk and branches of mountain almond trees (*Amygdalus scoparia* from *Rosaceae* family), which mainly grow in central parts of Iran (Kashki & Amirabadizadeh, 2011). Few studies have been devoted to investigating Zedo gum. Thus, the structural and functional properties of the Iranian native gum are unknown. A quick search on the Internet demonstrates that Zedo gum is mistakenly referred to as gum arabic in some texts and papers (Ghasempour, Alizadeh, & Bari, 2012).

It is well known that the functional properties of polysaccharides are related to their structure and molecular weight (Yang, Jiang, Zhao, Shi, & Wang, 2008). Several approaches have been used to contribute to the structural elucidation of polysaccharides, such as elemental analysis, monosaccharide measurement (by chromatography) and chemical group determination (by Fourier transform infrared spectroscopy/FTIR) (Alijani, Balaghi, & Mohammadifar, 2011; Luo et al., 2012). Other methods including LC-mass spectrometry are also developed to determine polysaccharide linkage and branching and to identify monosaccharides (Van Langenhove & Reinhold, 1985).

The molecular weight of a polymer is of prime importance in its applications and can be determined by various methods based on colligative properties such as light scattering and viscosity (Biesenberger & Sebastian, 1983). In recent years, GPC coupled with multi-angle laser light scattering (MALLS) detector has been demonstrated to be a powerful tool for analysis of polydispersed

* Corresponding author. Tel.: +98 2122648120; fax: +98 2122376470.
E-mail address: mohamdif@ut.ac.ir (M.A. Mohammadifar).

0144-8617/$ – see front matter © 2013 Elsevier Ltd. All rights reserved.
http://dx.doi.org/10.1016/j.carbpol.2013.09.095

polymers such as gum tragacanth (Mohammadifar, Musavi, Kiumarsi, & Williams, 2006) and gum arabic (Hassan, Al-Assaf, Phillips, & Williams, 2005). The technique is based on the absolute detection of light scattered from all the eluted fractions of the polymer after GPC separation (Picton, Bataille, & Muller, 2000). Some researchers have used colorimetric systems to describe a relationship between polysaccharides' color and their quality characteristics (Balaghi, Mohammadifar, & Zargaraan, 2010).

One of the most important functional features of polysaccharides is the control of solution and dispersion rheology, which is attributed to their high molecular weight, chain entanglement and polymer–solvent interactions (Khan, 1993). Therefore, rheological measurements have also become essential tools for characterizing component materials (Rafe, Razavi, & Farhoosh, 2013).

A complete insight into physical–chemical properties and structural features of Zedo gum is necessary to introduce its potential uses in food and other industries. Therefore, the objectives of this study were to determine the chemical composition, color parameters, rheological properties and thermal decomposition behavior of Zedo gum.

2. Materials and methods

2.1. Sample preparation and standards

Zedo gum was collected in plastic bags directly from the trees in Sirjan city, Kerman province. The gum was classified visually to three groups based on color (white, W; yellow, Y; and red, R). The gum samples were then powdered in a high-speed mechanical blender and sieved later to obtain uniform particle size of <500 μm.

The standards were from Sigma Aldrich Chemical Co. (St. Louis, MO, USA). The acids, bases, solvents and other chemicals were of analytical grade and from Merck (Darmstadt, Germany).

2.2. Color measurement

The L^* (lightness), a^* (redness) and b^* (yellowness) values and yellow index were determined for the gum powders using a Color-Eye 7000A reflectance spectrophotometer, which had d/8° geometry with a 6 inch integrating sphere and a pulsed xenon lamp. Reflectance data were collected over the full wavelength range of the instrument (360–750 nm with a 10 nm interval) with a specular component included through a small area view (SAV) aperture size. The results were expressed in accordance with the CIELAB system with reference to illuminant D65 and a visual angle of 10° (Balaghi et al., 2010).

2.3. Chemical composition analysis

Nitrogen, fat, ash and moisture content of the samples were determined using Official Methods of Analysis of Association of Official Analytical Chemist (AOAC International, 2005). The standard conversion factor of 6.25 was used to calculate crude protein content (Srichamroen & Chavasit, 2011). All the samples were analyzed three times for Na, K, Ca, Mg, Zn and Fe by an inductively coupled plasma atomic emission spectrometer (ICP-AES model Varian/Vista – pro CCD Simultaneous ICP-OES). Recoveries between 90% and 110% were accepted to validate the calibration. The results showed good agreement between the certified and analytical values and the recovery of the elements was partially complete for the most of them.

2.4. Gel permeation chromatography (GPC–MALLS)

GPC samples were prepared by mixing the powdered gums with deionized water on a magnetic stirrer for half an hour at 45 °C. The dispersions were kept refrigerated overnight, followed by centrifuging at 10,000 rpm (for 1 h at 4 °C); the supernatants were then freeze- dried. The soluble fractions were mixed with 0.1 M NaCl (2.0–3.0 g/l) and were kept at room temperature for 48 h. The solutions were filtered through a 1 μm filter, and a volume of 100 μl of the solutions was injected each time by an autosampler at 23 °C.

The molar mass and dispersity of the samples were determined using an Agilent system equipped with a PSS SECcurity 1100 HPLC-Pump, a PSS SECcurity 1100 Autosampler (Agilent 1100 Series) and a combination of four Suprema-Gel columns (PSS, D-55120 Mainz, Germany), a guard and three analytical ones (100, 1000 and 3000 Å). The eluent was 0.1 M NaCl at flow rate of 1 ml/min. A multi-angle laser light scattering detection system consisting of a PSS SLD 7000 MALLS detector (Brookhaven, BIC SLD 7000) with seven angles was also used. The GPC-software (PSS WinGPC Unity ver. 8.1) processed the output data including absolute values of number-average (M_n) and weight-average (M_w) molar mass. Dispersity was calculated as follows: $PD = M_w/M_n$, considering refractive index increment (dn/dc) of 0.141 ml/g.

2.5. Monosaccharide composition analysis

Glycosyl composition analysis was performed by combined gas chromatography/mass spectrometry (GC/MS) of the per-*O*-trimethylsilyl (TMS) derivatives of the monosaccharide methyl glycosides produced from the sample by acidic methanolysis (Inngjerdingen et al., 2012). Each sample (0.5–0.7 mg) was placed into a test tube and 20 μg of inositol was added to each sample as the internal standard. The samples were then frozen and lyophilized. Methyl glycosides were prepared from the dry samples by methanolysis in 1 M HCl in methanol at 80 °C (18 h) followed by re-*N*-acetylation with pyridine and acetic anhydride in methanol (for detection of amino sugars). The samples were then per-*O*-trimethylsilylated by treatment with Tri-Sil (Pierce) at 80 °C for half an hour (Merkle & Poppe, 1994). GC/MS analysis of the TMS methyl glycosides was performed on an Agilent 6890N GC interfaced to a 5975B MSD using a Supelco EC-1 fused silica capillary column (30 m × 0.25 mm ID).

2.6. Thermal analysis

TGA was carried out to determine thermal stability and rate of weight loss due to decomposition by a Perkin-Elmer Pyris Diamond TG/DTA analyzer at the heating rate of 10 °C/min and temperature range of 30–600 °C under nitrogen atmosphere (Adel, Abd El-Wahab, Ibrahim, & Al-Shemy, 2011). To obtain a more precise analysis of thermal stability, the software of the instrument calculated dm/dt or derivative thermogravimetry (DTG).

2.7. FTIR

FTIR spectra of the samples were recorded on a Perkin Elmer spectrometer (Spectrum One) in the frequency range of 4000–450 cm^{-1} and resolution of 4 cm^{-1} using the KBr pellet method. Deconvolution of the infrared spectra was performed using Perkin-Elmer software.

2.8. Rheological measurement

To prepare the dispersion of 2% (w/w), the gum powder was mixed with deionized water at 45 °C on a magnetic stirrer for approximately half an hour. The dispersions were kept in the refrigerator at 3 °C over night to hydrate completely. Rheological measurements were performed with a Physica MCR 301 rheometer (Anton-Paar, GmbH, Graz, Austria), using a Concentric Cylinder

CC27 system (26.665 mm in diameter). The temperature was controlled by a Peltier system equipped with a fluid circulator. The dispersions were left standing for 5 min to allow structure recovery and temperature equilibration. All the experiments were carried out at 25 ± 0.01 °C and a solvent trap was used to prevent evaporation. Flow curves were obtained over a shear rate range of 0.001–1000 s^{-1}. The Ostwald-de Waele and Cross models were fitted to the experimental data over a moderate and wide range of shear rates, respectively.

Strain sweep tests were done (0.01–1000%; 1 Hz) to determine the following parameters: (1) limiting value of the linear viscoelastic range (LVE or γ_L); (2) structural strength (η^* at LVE) and (3) damping factor ($\tan\delta$) to provide a direct view of whether the samples behaved as liquid or solid. Frequency sweep tests were performed using a frequency ramp from 0.01 to 100 Hz (Balaghi, Mohammadifar, Zargaraan, Gavlighi, & Mohammadi, 2011). Second log polynomial model (Eq. (1)) was fitted to frequency sweep data to obtain (b) and (c) coefficients as measures of frequency dependency of elastic modulus at low and high frequencies, respectively. Similarly, b' and c' (Eq. (2)) were measured for loss modulus:

$$G' = a\omega^{b}\omega^{c\ln\omega} \quad (1)$$

$$G'' = a'\omega^{b'}\omega^{c'\ln\omega} \quad (2)$$

where ω is angular frequency (rad/s).

2.9. Statistical analysis

The reported data in all the tables are means of triplicate observations. Analysis of Variance (ANOVA) was used for the data analysis (SPSS, 16). When F-values were significant ($p < 0.05$) in ANOVA, Duncan's multiple range test was used to compare the treatment means. The experimental data were fitted to rheological models using the Anton Paar Rheoplus software (Rheoplus/32V3.21).

3. Results and discussion

3.1. Color measurement

Color measurement was done to reveal the relationship of gum color and its quality or functional properties. The highest value of lightness (91.68) was found for sample W and ascending values of redness (a^*), yellowness (b^*) and yellow index were found for W, Y and R, respectively. Yellow indices of Y and R were about two and three times more than that of W. The color differences among the samples were statistically significant ($p < 0.001$). Therefore, the color differences confirmed that the present classification properly divided the gum to three distinct groups. Although the color of the gum tragacanth has been also used as a measure of quality classification criteria in traditional trades, a research on six species of the gum showed that color alone was not an appropriate measure of gum quality in terms of increasing viscosity (Balaghi et al., 2010).

3.2. Chemical composition

Table 1 shows chemical composition of the Zedo samples and gum arabic. Although Zedo gum with different colors can be harvested from one tree at the same time, some differences exist in their components. The protein and ash values were low and quite different from the reported values for gum arabic (Yebeyen, Lemenih, & Feleke, 2009). All the samples had different values for Na, K, Fe and Zn. Calcium, which is known to be responsible for gel formation in some plant gum exudates (Mhinzi, Mghweno, & Buchweishaija, 2008), was the main cation in the samples. Samples W and R showed no difference in terms of Mg content. Iron and sodium levels of the gum were lower than the ones found in gum arabic (Yebeyen et al., 2009) and Leucaena leucocephala gums (Rincon, Clamens, Guerrero, Leon De Pinto, & Martinez, 2007).

3.3. Monosaccharide composition and molecular weight

Sugar compositions of Zedo samples and gum arabic are shown in Table 2. Samples W and Y had the highest and lowest levels of total sugar content, respectively, which were higher than that of gum arabic. All the samples mainly consisted of galactose and arabinose, an indication of arabinogalactan polysaccharide. Fucose (Fuc), glucose (Glc), N-acetyl galactosamine (GalNAc) and N-acetyl glucosamine (GlcNAc) were not detected. Although gum arabic and Zedo gum are both classified as arabinogalactan polysaccharides, Zedo samples contained more arabinose (more than two times), less galactose and very little rhamnose and galacturonic acid. There are noticeable variations in sugar compositions of gums obtained from important *Acacia* species (gum arabic) including *A. senegal* and *A. seyal* but the absence of mannose, xylose and galacturonic acid is what they have in common (Islam, Phillips, Sljivo, Snowden, & Williams, 1997). However, some unusual data on gum arabic were also reported in which rhamnose and galactose were the main sugars (Cui & Mazza, 1996). It should be noted that the presence of xylose (6.8–9.2 mol%) and mannose (0.3–0.4 mol%) in Zedo samples can be used to distinguish these gums from arabic one. Arabinogalactans are found in most higher plants such as Arabidopsis leaf (Tryfona et al., 2012), carrot, maize and tomato, usually in glycoprotein form (Showalter, 2001) while Zedo gum samples contained too little protein to be considered a glycoprotein (Table 1). As far as we know, the United States FDA has approved larch arabinogalactan as an excellent source of dietary fiber (Kelly, 1999).

Molecular weight parameters (M_n, M_w and M_w/M_n) and radius of gyration (R_g) of the samples were also determined (Table 2). The results showed that W had the highest values of M_w and M_n while its PDI was the lowest. Considering molecular weights of the samples (W > Y > R) along with PDI values, it can be concluded that W consisted of heavier and more homogenous molecules. Sample R had an M_w of about 2.59×10^6 Da along with PDI of 4.05, which indicated a very heterogenous polysaccharide with low average molecular weight. The results indicated that the molecules of samples W and Y were more homogenous with higher weight average molecular weights (M_w), compared to gum arabic. In contrast to these findings, PDI value of sample R was much more than other samples and gum arabic. As other studies have demonstrated the strong impact of the molecular characteristics on polysaccharide functionalities (Hou et al., 2012), the differences in molar mass of the samples could be assumed as a major cause of different properties shown in this work.

3.4. TG/DTG

Thermal analysis signals of the samples had similar trends but different values. There were two distinct regions of weight loss on TGA curves, which were attributed to dehydration around 40–140 °C and a fast thermal decomposition around 250–300 °C. These findings were similar to the results of some other studies on natural or modified gums (Cozic, Picton, Garda, Marlhoux, & Le Cerf, 2009; Zohuriaan & Shokrolahi, 2004). Sample W had the highest weight loss value due to dehydration.

On the DTG curves, two points existed at which the weight loss reached the maximum rate. The DTG curves also showed predominance of a decompositional process in the second degradation step, which was similar to findings for xanthan gum (Faria et al., 2011). The highest loss rate in the first and second points belonged to the samples R and Y, respectively. Although no significant differences were observed among the temperatures at which the loss

Table 1
Chemical composition of the Zedo gum samples with different colors and gum arabic.

Sample	Protein (%)	Ash (%)	Moisture (%)7	Na (ppm)	K (ppm)	Ca (ppm)	Mg (ppm)	Zn (ppm)	Fe (ppm)
W	0.2141[a]	1.6750[a]	12.0885[a]	15[a]	1520[a]	6900[a]	950[a]	3[a]	7.8[a]
Y	0.2071[a]	1.5877[b]	11.2879[b]	9.7[b]	1670[b]	6900[a]	720[b]	1.5[b]	9.3[b]
R	0.1971[b]	1.3624[c]	12.1974[a]	1.1[c]	1480[a]	6300[b]	930[a]	1.2[c]	8.8[c]
GA[E]	2.18[c]	3.56[d]	15[c]	140[d]	–	7000[a]	2010[c]	ND	10[d]

[E] Gum Arabic. Values for GA reported by Yebeyen et al. (2009).
Values with different letters in each column are significantly different.

Table 2
Sugar compositions and molecular parameters of the Zedo gums and gum arabic (GA).

Sample	M_w ($\times 10^6$ Da)	M_n ($\times 10^6$ Da)	PDI	R_g (nm)	Total sugar (%)	Monosaccharide composition (mol%)						
						Ara	Rha	Xyl	GlcA	Man	Gal	4-O-Me-GlcA
W	4.74[a]	4.54[a]	1.04[a]	58[a]	98.4[a]	61.1[a]	1.1[a]	6.8[a]	0.6[a]	0.3[a]	28.4[a]	1.7[a]
Y	4.49[b]	3.68[b]	1.22[b]	56[a]	93.1[b]	62.8[b]	0.9[b]	6.7[a]	0.4[b]	0.3[a]	27.2[b]	1.7[a]
R	2.59[c]	0.65[c]	4.05[c]	48[b]	95.1[b]	54.5[c]	1.5[c]	9.2[b]	0.4[b]	0.4[b]	31.9[c]	2.1[b]
GA[E]	1.59[d]	0.67[c]	2.37[b]	24[c]	85.7[c]	27[d]	13[d]	–	14.5[d]	–	44[d]	1.5[d]

[E] Molecular parameters are reported by Siddig, Osman, Al-Assaf, Phillips, and Williams (2005), total sugar by Cui and Mazza (1996) and monosaccharides by Phillips and Williams (2000).
Values with different letters in each column are significantly different.

Table 3
Thermogravimetric data obtained during heating of Zedo gums and gum arabic (GA).

Samples	Loss due to dehydration (%)	Max. loss rate (μg/min)		Temperature (°C) at max. loss rate		Final residue (%) (600 °C)
		1st	2nd	1st	2nd	
W	10[a]	203.3[a]	273.1[a]	252.1[a]	304[a]	20.3[a]
Y	8[b]	332.8[b]	727.1[b]	255[a]	302.1[a]	23.3[b]
Z	8[b]	409.7[c]	471.1[c]	251[a]	302.2[a]	15.6[c]
GA[E]	13[c]	–	–	~280[b]	~305[a]	26[d]

[E] Reported by Cozic, Picton, Garda, Marlhoux, and Le Cerf (2009).
Values with different letters in each column are significantly different.

rate was at the maximum level, the white sample showed lower values, because of higher thermal stability (Table 3). Comparing the thermal analysis results with those reported for gum arabic (Cozic et al., 2009) revealed differences in some parameters.

3.5. FTIR

All the signals in the spectra were between 10%T and 65%T, which coincided with the optimum sample concentration and pellet thickness. Thirteen peaks were recognized on each spectrum. Two characteristic peaks of polysaccharides were observed at approximately 3424 and 2928 cm^{-1}, which were assigned to stretching vibration modes of O—H bound to carbons and asymmetric —CH_2— functional groups, respectively (Fan et al., 2012; Qiao et al., 2010). A stronger O—H band often overlapped the N—H region (near 3350 cm^{-1}) and the N—H stretches appeared as shoulders or peaks on the broader portion of the O—H band. In the C≡C region, a weak peak (2140 cm^{-1}) was observed. All the samples contained a moderately strong band at approximately 1620 cm^{-1}, which was partially associated with intramolecularly bound water and partially due to the presence of a carboxyl group. The band at 1375 cm^{-1} could be attributed to the bending group of symmetric —CH_3 (Derrick, Stulik, & Landry, 1999).

The wavenumber range between 1500 and 500 cm^{-1} represents the so-called carbohydrate fingerprints (Alijani et al., 2011). The peak at 1429 cm^{-1} was attributed to —COO— due to carboxylate groups of uronic acid residues (Vinod, Sashidhar, Sarma, & Vijaya Saradhi, 2008) and the peak at approximately 1230 cm^{-1} was assigned to stretching C—O in an acetyl group (Popescu, Larsson, Olaru, & Vasile, 2012). In addition, the peaks between 1200 and 1000 cm^{-1} were attributed to the complex band of C—O and C—C and those between 1000 and 700 cm^{-1} were attributed to C—H (Mitić, Nikolić, Cakić, Premović, & Ilić, 2009).

3.6. Rheological findings

3.6.1. Flow curves

Fig. 1 illustrates the dependence of viscosity on shear rate for all Zedo gum samples. Compared to the reports on the Newtonian flow behavior of gum arabic solutions up to 40% concentration (İbanoğlu, 2002), all Zedo gum samples showed a shear thinning behavior even at concentrations as low as 2% (w/w).

The power law model which provides a reasonable representation of many practical shear-thinning fluids (Gratão, Silveira, & Telis-Romero, 2007) was satisfactorily fitted to the

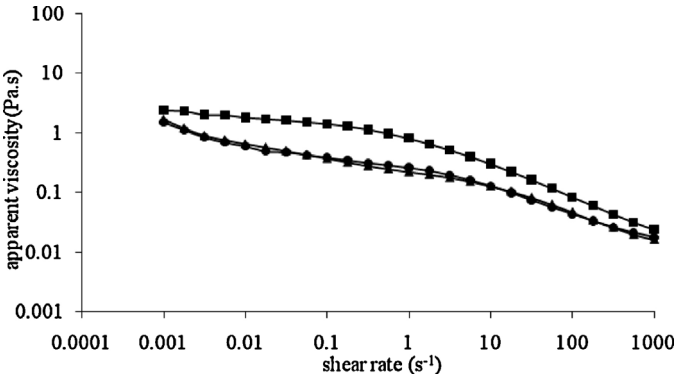

Fig. 1. Apparent viscosity versus shear rate of 2% (w/w) Zedo gum dispersions in deionized water at 25 °C: white (squares), yellow (triangles), red (circles).

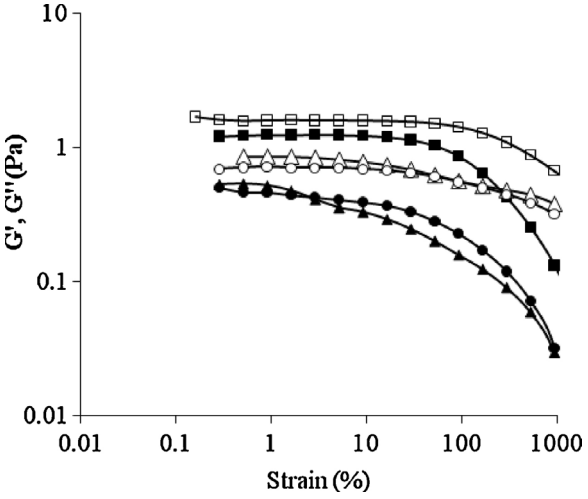

Fig. 2. G' (filled symbols) and G'' (open symbols) versus strain for Zedo gum samples of 2% (w/w) dispersions with different colors in deionized water at 25 °C: squares (W), triangles (Y) and circles (R).

Table 4
Power law parameters and Cross model parameters for zedo gum dispersions 2% (w/w) in deionized water.

Sample	Power low ($\tau = m\dot{\gamma}^n$)			Cross ($\left(\frac{\eta-\eta_\infty}{\eta_0-\eta_\infty} = \frac{1}{(1+(k\dot{\gamma})^m}\right)$)			
	m (Pa s)	n	R^2	η_0 (Pa s)	a	p	R^2
W	1.03[a]	0.45[a]	0.999	1.82[a]	1.23[a]	0.62[a]	0.999
Y	0.33[b]	0.56[b]	0.995	0.26[b]	0.57[b]	0.54[b]	0.995
R	0.33[b]	0.56[b]	0.993	0.36[c]	0.46[c]	0.67[c]	0.999

Values with different letters in each column are significantly different.

Table 5
Limiting value of strain (γ_L), loss tangent value ($\tan\delta_{LVE}$), complex viscosity (η^*_{LVE}) for Zedo gum dispersions (2%, w/w) as determined by strain sweep tests and parameters obtained from Eqs. (1) and (2) for the frequency sweep tests.

Sample	γ_L (%)	$\tan\delta_{LVE}$	η^*_{LVE}	b	c	b'	c'
W	46.8[a]	1.44[a]	0.29[a]	0.78[a]	−0.023[a]	0.63[a]	−0.034[a]
Y	2.59[b]	2[b]	0.15[b]	0.72[b]	0.007[b]	0.63[a]	0.004[b]
R	12.9[c]	1.8[c]	0.12[c]	0.86[c]	−0.035[c]	0.69[c]	0.027[c]

Values with different letters in each column are significantly different.

experimental data over the shear rate range of 0.001–1000 s^{-1} ($0.993 \leq R^2 \leq 0.999$) and the resulted consistency coefficient (m) and flow behavior index (n) were reported in Table 4. Results also indicated that both m and n values of W sample were significantly different from those of the two others. This was in agreement with the reported correlations between molecular weight of polysaccharides and power-law parameters. (Gillis et al., 2013; Hou et al., 2012).

3.6.2. Strain sweep

Strain sweep tests were conducted to discriminate the following two regions: a linear viscoelastic region (LVE), in which G' (elastic modulus) and G'' (loss modulus) were practically constant and deformation in the structure was reversible (small deformation), and a nonlinear region, in which G' and G'' began to decrease with increasing strain (large deformations). The structural character of the samples in the LVE range was expressed by comparing values of G' and G''. If $G' > G''$, a solid viscoelastic characteristic was present (gel characteristic) and, if $G'' > G'$, then a liquid viscoelastic characteristic (sol characteristic) was present (Hatami, Nejatian, & Mohammadifar, 2012).

As shown in Fig. 2, G'' was greater than G' over the tested range of strain for all the samples. As the viscose behavior dominated the elastic one (loss tangent > 1), it was expected from the samples to exhibit zero shear viscosity rather than yield point and

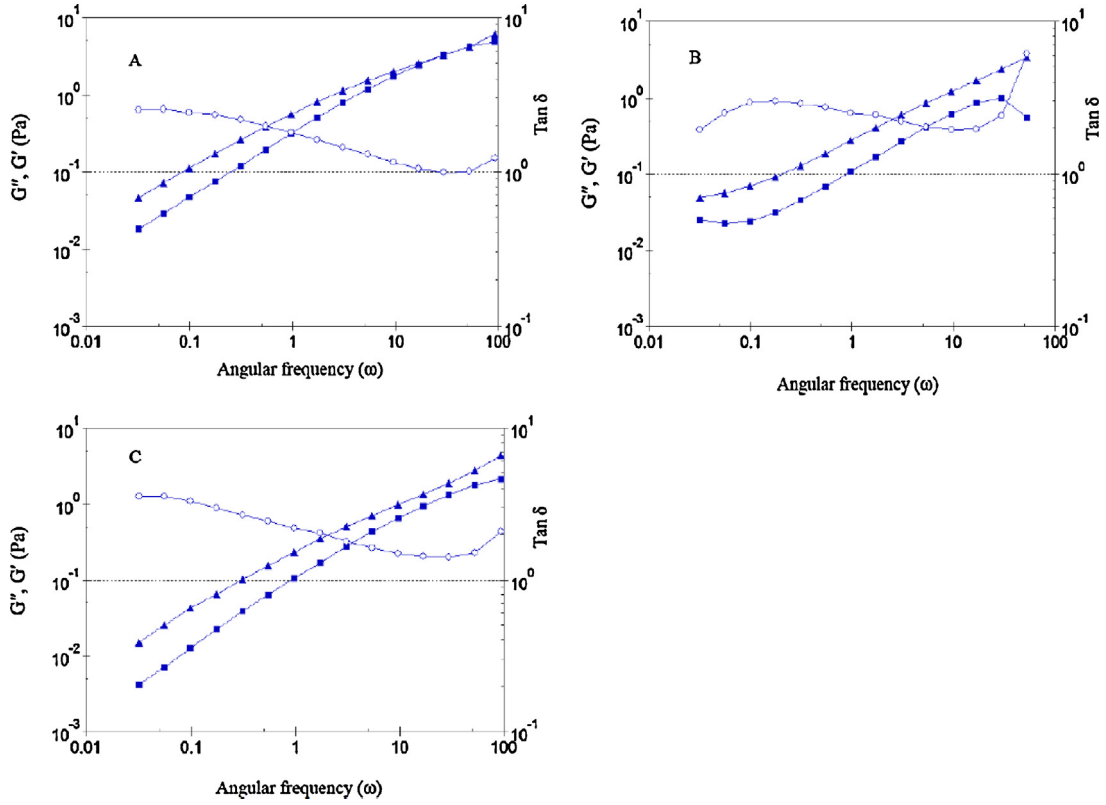

Fig. 3. G' (squares), G'' (triangles) and Damping factor (circles) of (A) sample W, (B) sample Y and (C) sample R as a function of angular frequency.

crossover point (flow point). However, to support this idea, it was required to perform frequency sweep test and study the shape of phase angle curve. The complex viscosity over the LVE range (η^*_{LVE}), limiting value of strain (γ_L) and loss tangent value ($\tan\delta_{LVE}$) of the three samples are shown in Table 5. γ_L was high for W which indicated that the sample had longer LVE ranges and implied a higher stability of the viscoelastic material under the γ-amplitude. Complex viscosity and loss tangent are important parameters for investigating the storage stability of dispersions (Pongsawatmanit, Temsiripong, & Suwonsichon, 2007). The higher value of complex viscosity, together with the lower value of loss tangent indicated more consistency and elastic behavior for this sample at moderate time scale.

3.6.3. Frequency sweep

Fig. 3 shows that G'' was larger than G' over the entire experimental frequency range; but, they approached each other at higher frequencies. No crossover point was found for samples Y and R in the range. However, at a rapid motion, they behaved more inflexibly and rigidly. During the shorter time scales (with the increase of angular frequency), the two moduli got close to each other and a crossover point occurred ($G'' = G'$) at angular frequency of about 26.58 rad/s for sample W (Fig. 3). Frequency sweep pattern of the polymer solutions depends on many factors like the concentration of the polymer, molecular weight, dispersity, structural properties (degree of branching, type and variety of functional groups and rigidity of backbone) and quality of solvent (Lapasin & Pricl, 1995). It seems that all the samples had a frequency sweep pattern similar to that of unlinked polymers, which usually occurred in dilute solutions. When the solution concentration of unlinked polymers is high enough, the polymer chains begin to form entanglements (Belitz, Grosch, & Schieberle, 2009). These entanglements are more likely to be mechanical interactions than chemical or physical–chemical bonds. Consequently, macromolecules are able to move slowly, even under small shear force, and glide along each other, showing partial or even complete disentanglement. According to the model parameters (b, b', c and c') in Table 5, R had higher deviation from a simple Maxwellian liquid. This could be related to its higher dispersity in comparison to that of W and Y. Considering the fact that the value of crossover frequency depends on the average molar mass, the occurrence of crossover point at higher frequency implied that sample W had the highest average molar mass among the studied samples. Loss tangent curves in Fig. 3 confirmed the mentioned trend and the transition from a predominantly viscous response at longer time scales toward a predominantly elastic response at shorter time scales (rubbery). The behavior of these dispersions can be compared with those of *Astragalus parrawianus*, *Astragalus floccosus* (Balaghi et al., 2011) and deacetylated *Sterculia striata* polysaccharide (Brito, Sierakowski, Reicher, Feitosa, & de Paula, 2005). However, the dynamic mechanical spectra of Zedo gum were different from those of some other gums with arabinogalactan structure like gum arabic (Li et al., 2009), peach tree gum exudates (Simas-Tosin et al., 2010) and Cashew-nut tree gum exudates (Pereira-Netto et al., 2007).

4. Conclusion

Sugar analysis revealed that Zedo gum was an arabinogalactan polysaccharide. Based on the color measurements, three different types of Zedo gum were identified which had some different properties. All the samples showed similar FTIR patterns. They had a non-Newtonian behavior and frequency sweep pattern similar to those of unlinked polymers. Higher values of thermal stability, molecular weight, total carbohydrate, sodium and zinc content and apparent viscosity belonged to sample W. Comparison of the obtained data with the previously reported results for gum arabic indicated that these two arabinogalactan polysaccharides differed greatly.

Acknowledgments

We would like to acknowledge the financial support by Robertet Sirjan Company and appreciate its managing director, Mr. Kamal S. Tehrani, for all his constant help and encouragement during this research.

References

Adel, A. M., Abd El-Wahab, Z. H., Ibrahim, A. A., & Al-Shemy, M. T. (2011). Characterization of microcrystalline cellulose prepared from lignocellulosic materials Part II: Physicochemical properties. *Carbohydrate Polymers*, *83*(2), 676–687.

Alijani, S., Balaghi, S., & Mohammadifar, M. A. (2011). Effect of gamma irradiation on rheological properties of polysaccharides exuded by *A. fluccosus* and *A. gossypinus*. *International Journal of Biological Macromolecules*, *49*(4), 471–479.

AOAC International. (2005). *Official methods of analysis of AOAC international* (18th ed.). Maryland: Association of Official Analytical Chemist.

Balaghi, S., Mohammadifar, M. A., & Zargaraan, A. (2010). Physicochemical and rheological characterization of gum tragacanth exudates from six species of Iranian Astragalus. *Food Biophysics*, *5*(1), 59–71.

Balaghi, S., Mohammadifar, M. A., Zargaraan, A., Gavlighi, H. A., & Mohammadi, M. (2011). Compositional analysis and rheological characterization of gum tragacanth exudates from six species of Iranian Astragalus. *Food Hydrocolloids*, *25*(7), 1775–1784.

Belitz, H., Grosch, W., & Schieberle, P. (2009). *Food chemistry* (4th revised and extended edn.). Heidelberg: Springer.

Biesenberger, J. A., & Sebastian, D. H. (1983). *Principles of polymerization engineering*. Wiley.

Cozic, C., Picton, L., Garda, M.-R., Marlhoux, F., & Le Cerf, D. (2009). Analysis of arabic gum: Study of degradation and water desorption processes. *Food Hydrocolloids*, *23*(7), 1930–1934.

Cui, S. W. (2005). *Food carbohydrates: Chemistry, physical properties and applications*. Boca Raton: CRC Press.

Cui, W., & Mazza, G. (1996). Physicochemical characteristics of flaxseed gum. *Food Research International*, *29*(3–4), 397–402.

De Brito, A. C. F., Sierakowski, M. R., Reicher, F., Feitosa, J. P. A., & de Paula, R. C. M. (2005). Dynamic rheological study of Sterculia striata and karaya polysaccharides in aqueous solution. *Food Hydrocolloids*, *19*(5), 861–867.

Derrick, M. R., Stulik, D., & Landry, J. M. (1999). *Infrared spectroscopy in conservation science – scientific tools for conservation*. Los Angeles: J. Paul Getty Trust.

Fan, L., Cao, M., Gao, S., Wang, W., Peng, K., Tan, C., et al. (2012). Preparation and characterization of a quaternary ammonium derivative of pectin. *Carbohydrate Polymers*, *88*(2), 707–712.

Faria, S., de Oliveira Petkowicz, C. L., de Morais, S. A. L., Terrones, M. G. H., de Resende, M. M., de França, F. P., et al. (2011). Characterization of xanthan gum produced from sugar cane broth. *Carbohydrate Polymers*, *86*(2), 469–476.

Ghasempour, Z., Alizadeh, M., & Bari, M. R. (2012). Optimisation of probiotic yoghurt production containing Zedo gum. *International Journal of Dairy Technology*, *65*(1), 118–125.

Gillis, R. B., Adams, G. G., Wolf, B., Berry, M., Besong, T. M. D., Corfield, A., et al. (2013). Molecular weight distribution analysis by ultracentrifugation: Adaptation of a new approach for mucins. *Carbohydrate Polymers*, *93*(1), 178–183.

Gratão, A. C. A., Silveira, V., Jr., & Telis-Romero, J. (2007). Laminar flow of soursop juice through concentric annuli: Friction factors and rheology. *Journal of Food Engineering*, *78*(4), 1343–1354.

Hassan, E. A., Al-Assaf, S., Phillips, G. O., & Williams, P. A. (2005). Studies on Acacia gums: Part III molecular weight characteristics of *Acacia seyal* var. seyal and *Acacia seyal* var fistula. *Food Hydrocolloids*, *19*(4), 669–677.

Hatami, M., Nejatian, M., & Mohammadifar, M. A. (2012). Effect of co-solute and gelation temperature on milk protein and gum tragacanth interaction in acidified gels. *International Journal of Biological Macromolecules*, *50*(4), 1109–1115.

Hou, Z., Zhang, M., Liu, B., Yan, Q., Yuan, F., Xu, D., et al. (2012). Effect of chitosan molecular weight on the stability and rheological properties of β-carotene emulsions stabilized by soybean soluble polysaccharides. *Food Hydrocolloids*, *26*(1), 205–211.

İbanoğlu, E. (2002). Rheological behaviour of whey protein stabilized emulsions in the presence of gum arabic. *Journal of Food Engineering*, *52*(3), 273–277.

Inngjerdingen, K. T., Meskini, S., Austarheim, I., Ballo, N., Inngjerdingen, M., Michaelsen, T. E., et al. (2012). Chemical and biological characterization of polysaccharides from wild and cultivated roots of Vernonia kotschyana. *Journal of Ethnopharmacology*, *139*(2), 350–358.

Islam, A., Phillips, G., Sljivo, A., Snowden, M., & Williams, P. (1997). A review of recent developments on the regulatory, structural and functional aspects of gum arabic. *Food Hydrocolloids*, *11*(4), 493–505.

Kashki, M. T., & Amirabadizadeh, H. (2011). Approach to plant communities in desert regions of Khorasan province in Iran. *international Journal of Science and Nature*, *2*(1), 42–46.

Kelly, G. S. (1999). Larch arabinogalactan: Clinical relevance of a novel immune-enhancing polysaccharide. *Alternative Medicine Review: A Journal of Clinical Therapeutic*, *4*(2), 96–103.
Khan, R. (1993). *Low calorie foods & food ingredients*. Springer.
Lapasin, R., & Pricl, S. (1995). *Rheology of industrial polysaccharides: Theory and applications*. Blackie Academic & Professional London.
Li, X., Fang, Y., Al-Assaf, S., Phillips, G. O., Nishinari, K., & Zhang, H. (2009). Rheological study of gum arabic solutions: Interpretation based on molecular self-association. *Food Hydrocolloids*, *23*(8), 2394–2402.
Luo, Q., Sun, Q., Wu, L., & Yang, Z. (2012). Structural characterization of an immunoregulatory polysaccharide from the fruiting bodies of Lepista sordida. *Carbohydrate Polymers*.
Merkle, R. K., & Poppe, I. (1994). Carbohydrate composition analysis of glycoconjugates by gas-liquid chromatography/mass spectrometry. In G. W. H. William, & J. Lennarz (Eds.), *Methods in enzymology* (Vol. 230) (pp. 1–15). Academic Press.
Mhinzi, G. S., Mghweno, L. A. R., & Buchweishaija, J. (2008). Intra-species variation of the properties of gum exudates from two Acacia species of the series Gummiferae. *Food Chemistry*, *107*(4), 1407–1412.
Mitić, Ž., Nikolić, G. S., Cakić, M., Premović, P., & Ilić, L. (2009). FTIR spectroscopic characterization of Cu(II) coordination compounds with exopolysaccharide pullulan and its derivatives. *Journal of Molecular Structure*, *924–926*, 264–273.
Mohammadifar, M. A., Musavi, S. M., Kiumarsi, A., & Williams, P. A. (2006). Solution properties of targacanthin (water-soluble part of gum tragacanth exudate from *Astragalus gossypinus*). *International Journal of Biological Macromolecules*, *38*(1), 31–39.
Pereira-Netto, A. B., Pettolino, F., Cruz-Silva, C. T. A., Simas, F. F., Bacic, A., Carneiro-Leão, A. M. D. A., et al. (2007). Cashew-nut tree exudate gum: Identification of an arabinogalactan-protein as a constituent of the gum and use on the stimulation of somatic embryogenesis. *Plant Science*, *173*(4), 468–477.
Persin, Z., Stana-Kleinschek, K., Foster, T. J., van Dam, J. E. G., Boeriu, C. G., & Navard, P. (2011). Challenges and opportunities in polysaccharides research and technology: The EPNOE views for the next decade in the areas of materials, food and health care. *Carbohydrate Polymers*, *84*(1), 22–32.
Phillips, G. O., & Williams, P. A. (2000). *Handbook of hydrocolloids*. CRC Press.
Picton, L., Bataille, I., & Muller, G. (2000). Analysis of a complex polysaccharide (gum arabic) by multi-angle laser light scattering coupled on-line to size exclusion chromatography and flow field flow fractionation. *Carbohydrate Polymers*, *42*(1), 23–31.
Pongsawatmanit, R., Temsiripong, T., & Suwonsichon, T. (2007). Thermal and rheological properties of tapioca starch and xyloglucan mixtures in the presence of sucrose. *Food Research International*, *40*(2), 239–248.
Popescu, C.-M., Larsson, P. T., Olaru, N., & Vasile, C. (2012). Spectroscopic study of acetylated kraft pulp fibers. *Carbohydrate Polymers*, *88*(2), 530–536.
Qiao, D., Liu, J., Ke, C., Sun, Y., Ye, H., & Zeng, X. (2010). Structural characterization of polysaccharides from *Hyriopsis cumingii*. *Carbohydrate Polymers*, *82*(4), 1184–1190.
Rafe, A., Razavi, S. M. A., & Farhoosh, R. (2013). Rheology and microstructure of basil seed gum and β-lactoglobulin mixed gels. *Food Hydrocolloids*, *30*(1), 134–142.
Rincon, F., Clamens, C., Guerrero, R., Leon De Pinto, G., & Martinez, M. (2007). Physicochemical characterizatin of gum exudate from Leucaena Leucocephala located in Venezuela. *Boltin Del Centro De Investigaciones Biologicas*, *41*(3), 323–330.
Showalter, A. M. (2001). Arabinogalactan-proteins: Structure, expression and function. *Cellular and Molecular Life Sciences*, *58*(10), 1399–1417.
Siddig, N. E., Osman, M. E., Al-Assaf, S., Phillips, G. O., & Williams, P. A. (2005). Studies on acacia exudate gums, part IV. Distribution of molecular components in *Acacia seyal* in relation to *Acacia senegal*. *Food Hydrocolloids*, *19*(4), 679–686.
Simas-Tosin, F. F., Barraza, R. R., Petkowicz, C. L. O., Silveira, J. L. M., Sassaki, G. L., Santos, E. M. R., et al. (2010). Rheological and structural characteristics of peach tree gum exudate. *Food Hydrocolloids*, *24*(5), 486–493.
Srichamroen, A., & Chavasit, V. (2011). Rheological properties of extracted malva nut gum (*Scaphium scaphigerum*) in different conditions of solvent. *Food Hydrocolloids*, *25*, 444–450.
Tryfona, T., Liang, H.-C., Kotake, T., Tsumuraya, Y., Stephens, E., & Dupree, P. (2012). Structural characterization of arabidopsis leaf arabinogalactan polysaccharides. *Plant Physiology*, *160*(2), 653–666.
Van Langenhove, A., & Reinhold, V. N. (1985). Determination of polysaccharide linkage and branching by reductive depolymerization gas-liquid chromatography and gas-liquid chromatography-mass spectrometry reference data. *Carbohydrate Research*, *143*, 1–20.
Vinod, V. T. P., Sashidhar, R. B., Sarma, V. U. M., & Vijaya Saradhi, U. V. R. (2008). Compositional analysis and rheological properties of gum Kondagogu (*Cochlospermum gossypium*): A tree gum from India. *Journal of Agricultural and Food Chemistry*, *56*(6), 2199–2207.
Yang, B., Jiang, Y., Zhao, M., Shi, J., & Wang, L. (2008). Effects of ultrasonic extraction on the physical and chemical properties of polysaccharides from longan fruit pericarp. *Polymer Degradation and Stability*, *93*(1), 268–272.
Yebeyen, D., Lemenih, M., & Feleke, S. (2009). Characteristics and quality of gum arabic from naturally grown *Acacia senegal* (Linne) Willd. trees in the Central Rift Valley of Ethiopia. *Food Hydrocolloids*, *23*(1), 175–180.
Zohuriaan, M. J., & Shokrolahi, F. (2004). Thermal studies on natural and modified gums. *Polymer Testing*, *23*(5), 575–579.